Journal of Superconductivity, Vol. XXX, 1998

Tunneling and Photoemission in an SO(6) Superconductor

R.S. Markiewicz[a,b], C. Kusko[a,b,c], and M.T. Vaughn[a]

Received 1 June 1998

Combining the results of tunneling, photoemission and thermodynamic studies, the pseudogap is unambiguously demonstrated to be caused by Van Hove nesting: a splitting of the density of states peak at $(\pi, 0)$. The fact that the splitting remains symmetric about the Fermi level over an extended doping range indicates that the Van Hove singularity is pinned to the Fermi level. Despite these positive results, an ambiguity remains as to what instability causes the pseudogap. Charge or spin density waves, superconducting fluctuations, and flux phases all remain viable possibilities. This ambiguity arises because the instabilities of the two-dimensional Van Hove singularity are associated with an approximate SO(6) symmetry group, which contains Zhang's SO(5) as a subgroup. It has two 6-component superspins, one of which mixes Zhang's (spin-density wave plus d-wave superconductivity) superspin with a flux phase operator.
This is the smallest group which can explain striped phases in the cuprates.
Evidence for a prefered hole density in the charged stripes is discussed.

KEY WORDS: High-T$_c$ cuprates, underdoped, pseudogap, striped phases.

1. 11 YEARS of the VAN HOVE SCENARIO: REMINISCENCES of R.S.M.

Early work on the Van Hove model of high-T$_c$ superconductivity was criticized for a number of reasons, chiefly (1) the perfect nesting of the Fermi surface would cause instabilities which would overwhelm superconductivity; and (2) the Van Hove singularity (VHS) is associated with a special doping, and hence would require 'fine tuning' of the model parameters to fall at the Fermi level, whereas superconductivity exists over an extended doping range. In June, 1987, I suggested[1] the picture which has become the heart of the generalized Van Hove scenario[2]. First, introduction of next-nearest-neighbor hopping – t' (t_{OO}) in a one (three)-band model – would push the VHS off of half filling, leading to imperfect nesting, with residual hole pockets and ghost Fermi surfaces[3]. Secondly, this very sensitivity to instability could in turn lower the free energy precisely when the Fermi surface coincides with the VHS, thereby stabilizing this special doping – and that the reason superconductivity might persist over such an extended doping range is that the material is inhomogeneous, with one phase pinned at the VHS. Due to charging effects, such phase separation would be nanoscale[4].

While a microscopic model only appeared in 1989[5], I quickly found that the doping dependence of both resistivity and Hall effect could be understood in the context of a percolation model[3,6], and Bill Giessen and I noted that the Uemura plot[7] could be interpreted in terms of an *optimal doping* for each cuprate, which we identified with the pure VHS phase[8]. At the 1988 MRS Meeting, Jim Jorgensen asked me if the phase separation really had to be nanoscale, and I said it was a problem of the counterions: if the Sr in $La_{2-x}Sr_xCuO_4$ could be made mobile, there was no reason that a macroscopic phase separation couldn't occur – with one phase pinned at optimal doping. I didn't know then that Jim and co-workers had just discovered such a phase in $La_2CuO_{4+\delta}$, where the doping is due to mobile

(a) Physics Department and (b) Barnett Institute, Northeastern University, Boston, MA 02115, U.S.A. (c) On leave of absence from Inst. of Atomic Physics, Bucharest, Romania.

interstitial oxygens[9].

One problem was: just where is the VHS. A VHS at half filling could produce an antiferromagnetic instability with large pseudogap[10] but no hole pockets[11], while a VHS at finite doping could explain hole pockets and optimal doping, but not antiferromagnetism. I explored this issue by putting t' into a slave boson model, to separate Mott and nesting instabilities[5]. I found that the Mott instability – and hence the accompanying antiferromagnetism – remain locked to half filling, while for the VHS I found a striking surprise: *correlation effects pin the Fermi level close to the VHS over an extended doping range*, extending across the underdoped regime from half filling to optimal doping (close to the bare VHS). Numerous subsequent studies have confirmed the Van Hove pinning (cited on p. 1223 of Ref. [2]).

In this same paper[5], I demonstrated a viable mechanism for nanoscale phase separation: a charge-density wave (CDW) instability is strongly enhanced when the Fermi level coincides with the bare VHS, leading to a free energy minimum at optimal doping. Since the Mott instability produces a separate minimum at half filling, the energy is lowered by separating into the two end phases. This model was clearly distinguished from other models, in that there is a highly unusual and characteristic fractional hole doping of the hole rich phase (this doping fixed by the VHS), whereas all other models had a doped phase with one hole per Cu. Now I had an *embarras de richesses*: both pinning of the VHS by correlation effects and phase separation, which amounted to a different pinning mechanism. Put another way: were the cuprates characterized by phase separation or by the (pseudo)gap associated with nesting? I puzzled over this issue for a number of years, convinced that somehow both viewpoints were correct – rather like the particle vs wave problem in quantum mechanics. I was (and am) convinced that both the low-temperature orthorhombic (LTO) and low-temperature tetragonal (LTT) phases in LSCO was driven by this mechanism, and I introduced the concept of Van Hove-Jahn-Teller effect to explain the LTO phase as a dynamic Jahn-Teller (JT) phase[12,13]. But there was something missing: there should have been a tetragonal dynamic JT phase at higher temperatures. In the years from 1987-1991, I was often asked where was the evidence for a CDW or other nesting instability.

Things changed when I realized that the 'spin gap' and thermodynamic[14] data were consistent with a simple model for the pinned Van Hove phase [12,15]. New photoemission data[16] showed that the pseudogap is associated with the band dispersion near $(\pi, 0)$ – i.e., the locus of the VHS, while Tranquada, et al.[17] showed the presence of nanoscale phase separation in the form of stripes, which appeared to be suspiciously coextensive with the pseudogap regime. After writing an extensive review[2], I put my ideas together into a self-consistent three-band slave boson calculation, reported at the first Stripes Conference[18]. Correlation effects keep the Fermi level close to the VHS from half filling to optimal doping. Near half filling, correlation effects drive the Cu-O hopping to zero, and the remaining dispersion due to J has a VHS at half filling, and gains additional stability by splitting the VHS via a flux phase[18,19]. Doping restores the hopping, simultaneously introducing a strong electron-phonon coupling via modulation of the Cu-O separation, leading to a maximal CDW instability at optimal doping. The two instabilities in turn drive phase separation. Attempts to model this phase separation led to good fits to the doping dependence of the photoemission dispersion. There was an important prediction: the VHS is found in photoemission to be below the Fermi level, because it is *simultaneously above the Fermi level*: the pseudogap consists of a splitting of the VHS into two features at $(\pi, 0)$, but split in energy about the Fermi level. Photoemission could not reveal the upper VHS, but recent tunneling studies[20,21] fully confirm this prediction, as well as demonstrating that the lower peak coincides with the photoemission VHS feature.

At the mean-field level, the CDW has long-range order. However, when fluctuations are included in a mode-coupling scheme, there is only short-range order, with a real pseudogap opening up in the temperature range between the mean field transition temperature and a much lower transition to long-range order, driven by interlayer coupling[22]. If this interlayer coupling is absent, the CDW resembles a *quantum critical point* (QCP), with correlation length diverging as $\xi \sim T^{-1/2}$[22]. It is not a conventional QCP, in that in the absence of phase sepatation it is not the terminus of a finite temperature phase transition (i.e., there is no renormalized classical regime).

2. SUPERCONDUCTIVITY and TUNNELING

The three-band model[18] revealed that the striped phases are associated with two nesting instabilities, flux phase near half filling and CDW at optimal doping, leading to a large pseudogap near $(\pi, 0)$ and

simultaneously to nanoscale phase separation between magnetic and hole-doped stripes. In the LSCO system, adding Nd or replacing the Sr with Ba leads to long range stripe phase order[17] while suppressing superconductivity – clearly demonstrating that *three distinct phases* must be involved. In the one-band model[12,15] this situation is simplified by replacing the striped phase by a uniform CDW phase. The key approximation is the *Ansatz* of reducing the strong correlation effects and phase separation by their most important effect: the *pinning of the Fermi level to the VHS*, over the full doping range from half filling to optimal doping. In the overdoped regime, the simplest approximation is assumed: the band structure stops changing with doping, and the Fermi level shifts in a rigid band fashion.

Fig. 1. Phase diagram of pinned Balseiro-Falicov model. Circles = net tunneling gap, Δ_t. Inset: Tunneling spectra of a density-wave superconductor, using parameters of dotted line in main frame. Temperatures (from top to bottom) = 130, 110, 90, 80, 70, 50, and 30K (dashed lines: T above the superconducting transition temperature).

The pseudogap seen in tunneling measurements on $Bi_2Sr_2CaCu_2O_{8+\delta}$ (Bi-2212)[20,21] can be fit to this model. We have calculated the tunneling spectrum[23], Figure 1, and find a smooth evolution from pseudogap (CDW) phase to mixed CDW-superconductor. For a pure CDW, the spectral function is of BCS form:

$$A(k,\omega) = 2\pi[u_k^2\delta(\omega - E_{k+}) + v_k^2\delta(\omega - E_{k-})], \quad (1)$$

with $u_k^2 = 1 - v_k^2 = (1 + \epsilon_{k-}/\tilde{E}_k)/2$, $E_{k\pm} = (\epsilon_{k+} \pm \tilde{E}_k)/2$, $\epsilon_{k\pm} = \epsilon_k \pm \epsilon_{k+Q}$ and $\tilde{E}_k = \sqrt{\epsilon_{k-}^2 + 4G_k^2}$, where the nesting vector $Q = (\pi,\pi)$, and the gap G_k and dispersion ϵ_k are defined in Refs. [12,24]. The model involves three gap parameters, two (G_0 and G_1) associated with CDW order, and one Δ with superconductivity. Figure 1 shows the calculated phase diagram and the net low-T tunneling gap, defined as half the peak-peak separation. The inset shows that in the mixed CDW-superconducting state a single gap evolves in the calculated tunneling density of states $\rho(E)$ (except for phonon structure). The ratio of the total gap to the CDW/superconducting onset temperature is nearly doping independent, $2\Delta_t/k_BT^* \simeq 4.1$. Since we use the model of Balseiro and Falicov (BF)[24] to describe the underlying CDW-superconductivity competition, we refer to this as the *pinned BF* (pBF) model. At present, it involves s-wave superconductivity, but we are working on an SO(6) generalization, including d-wave superconductivity.

For tunneling along the c-axis into a two-dimensional material, the tunneling density of states (dos) is an average of the in-plane quasiparticle dos[25]. In this case, there is a one-to-one correspondence between features in the electronic band dispersion, as measured in photoemission, and peaks in the tunneling dos, Fig. 2. The main tunneling peaks (A) coincide with the split electronic energy dispersion near $(\pi,0)$ and $(0,\pi)$ of the Brillouin zone – and hence with the corresponding photoemission peaks, as found experimentally[21]. In the present BCS-like model, the slight discontinuity at the phonon energy produces a large peak in the tunneling spectrum (D). Note that at $(\pi,0)$ the CDW and superconducting gaps combine to form a single feature (A) in both photoemission and tunneling, whereas the gaps split into two separate features, B associated with superconductivity and C with the CDW, near $(\pi/2,\pi/2)$.

Fig. 2. Dispersion (a) and tunneling dos (b) near the Fermi level in the pBF model in the presence of combined CDW and superconducting order. Parameters are G_0 =7.45meV, G_1 =14.3meV, Δ =13.1meV; other parameters as in Ref. [23]. Dotted lines = ghost bands.

The presence of only a single, combined gap at $(\pi, 0)$ is a consequence of an underlying SO(6) symmetry of the VHS, as discussed in the following section. In turn, this explains the smooth evolution of the pseudogap into the superconducting gap, Fig. 1 insert, which therefore need not be taken as evidence for precursor pairing in the pseudogap phase.

A most exciting possibility is that by comparing the photoemission and tunneling data, one should be able to experimentally *measure* the pinning of the Fermi level to the VHS. Indeed, Renner, et al.[20], unaware of this prediction[2], have noted that 'the pseudogap is centered at the Fermi level in both under- and overdoped samples. It is therefore unlikely that the pseudogap results from a band structure effect.'

Fig. 3. Splitting of the Fermi level from the VHS, measured as the normalized difference between the tunneling and photoemission pseudogaps, $(\Delta_{PE} - \Delta_{TU})/\Delta_{TU}$. Solid line = theory in the absence of pinning; open circles = derived from data of Refs. [21,26]. Inset: tunneling dos at several dopings.

To quantify the extent of pinning, we test the null hypothesis. We compare the presently available data with the expected tunneling spectra for a pure d-wave superconductor in the absence of pinning, as doping is varied and the Fermi level passes through the VHS, Fig. 3. From the inset, it can be seen that the two peaks in tunneling are symmetric when the Fermi level is exactly at the VHS (optimal doping), while the peak on the photoemission (inverse photoemission) side is stronger for underdoped (overdoped) samples, in accord with experiment. However, for strong enough doping away from optimal, the peak should split, which is not seen. Since the superconducting gap shifts off of $(\pi, 0)$, we take the difference between the tunneling gap Δ_{TU} and the photoemission gap Δ_{PE} as an experimental measure of the splitting, Fig. 3. While there is considerable error, the splitting in overdoped samples is close to what is expected, *but the splitting is absent in underdoped samples* – strong evidence for Van Hove pinning.

3. SO(6)

A one-dimensional metal is susceptible to a variety of instabilities, including singlet or triplet superconductivity, CDW's and spin-density waves. These instabilities can be organized group-theoretically[27], either on the basis of a symmetry group, or in terms of a larger spectrum-generating algebra (SGA), which contains the hamiltonian as a group element, and hence can be used to generate the full energy spectrum. A similar analysis can be applied to the Van Hove scenario, in terms of an approximate SO(6) symmetry group, or SO(8) SGA[28].

This SO(6) group contains as subgroups Zhang's SO(5)[29], Yang and Zhang's SO(4)[30], and Wen and Lee's SO(3)[31] (SU(2)). It includes two 6-dimensional superspins, which form an 'isospin' doublet[28]: one combines Zhang's SO(5) superspin (antiferromagnetism plus d-wave superconductivity) and the flux phase; the other involves s-wave superconductivity and a CDW (as in the pBF model) with an exotic spin current phase. There is a most interesting evolution of these groups from one dimension to two, Table I. Lin, et al.[32] analyzed the group structure of a two-leg ladder. They found an SO(8) symmetry group, which involves the SO(6) group as a subgroup, plus operators which are antisymmetric for $\vec{k} \rightarrow -\vec{k}$. These latter operators are essential in the one-dimensional case, where the Fermi surface consists of two points $\pm k_{Fx}$, but are irrelevant for the VHS's, which are on the Brillouin zone boundary, and hence do not couple to these operators. Table I illustrates the evolution of a single superspin (Lin, et al.'s d-Mott state) from 1-D to 2-D. In this Table, SDW = spin-density wave; sc = superconductivity; S_{12}^z and P_{12} are symbols introduced by Lin, et al.[32] for two of their SO(8) operators, called band spin difference and relative band chirality; and a dash indicates that a corresponding operator is lacking. Note that the 1-D CDW connects k_F and $-k_F$, while the 2-D CDW discussed above connects $(\pi, 0)$ and $(0, \pi)$. Note further that the SO(6) structure persists down to lad-

Table I. Superspin vs. dimensionality

1-D	**ladder**	**2-D**
SDW	SDW	SDW
singlet sc	d-wave sc	d-wave sc
1-D CDW	P_{12}	—
—	S_{12}^z	flux phase

ders two cells wide, and hence should remain valid in describing the striped phases.

In the 1-D metals, the SGA aspect is more fundamental than the symmetry aspect. The various instabilities are usually not degenerate in energy, as required by a symmetry group. Instead, they are governed by the allowed interaction terms, g's – hence the name g-ology – and the object of research is to derive the allowed phase diagram as a function of the possible g-values. In this case, the SGA is useful in cataloging the allowed instabilities[27]. The situation is similar for the VHS. The one-band model is not itself symmetric under SO(6), but shows considerable signs of the underlying SO(8) SGA. Thus, the form of the phase diagram in Fig. 1 is generic of any competition between a nesting operator and a pairing operator, while the pseudogap at $(\pi, 0)$ has the simple form

$$\Delta_t = \sqrt{\Sigma_{i=1}^{12} \Delta_i^2}, \tag{2}$$

where the Δ_i's are the gaps associated with the twelve components of both superspin vectors[33]. When $t' = 0$, this vector addition of the gaps holds for the full Fermi surface. Note that for a symmetry group, all the Δ_i's in Eq. 2 would have equal magnitudes.

The corresponding 2-D G-ology phase diagram can be worked out[28,34], in analogy with the 1-D case. In the Hubbard limit, the only interaction is the U term, and the phase diagram has a natural evolution from SDW at half filling to d-wave superconductivity in the doped materials. However, this simple picture cannot account for the striped phases, which compete with superconductivity (e.g., at 1/8 doping, where there is long-ranged stripe order, superconductivity is suppressed). By adding a phonon-mediated effective electron-electron coupling, a CDW phase can be stabilized in the doped material, and competition between CDW and SDW generates a striped phase.

4. POSTSCRIPT: HOW WIDE ARE THE CHARGED STRIPES?

There was considerable discussion at the Conference as to whether the charged stripes were one cell wide or two cells wide (a.k.a.: site-centered or bond-centered). This may seem like a trivial issue, but it can have profound consequences: the nature of the striped phase at optimal doping, and ultimately the relevance of the t-J model to high-T$_c$ superconductivity.

The issues may be conveniently addressed by considering the White-Scalapino[35] model of the 1/8 doped state. The overall magnetic and charge orders are consistent with experiment[17], but our main concern here is the actual charge distribution. The charge periodicity is four CuO_2 cells across, with two magnetic cells having an average hole density of $\sim$ 0.07 holes per Cu, and two hole-doped cells, each containing $\sim$ 0.18 hole. Since the magnetic and hole-doped stripes have equal width, *this is the highest doping at which a magnetic domain wall model makes sense.* This is particularly true, since there is a strong tendency for the magnetic stripes to contain an even number of cells – since in that case, there can be a spin gap, as in an even-legged ladder[36]. Hence, as the doping is increased above 1/8, the magnetic cells can no longer shrink in width, and there must be a phase transition in the nature of the stripes. [If the hole-doped stripes were only one cell wide, this anomalous behavior would only arise near a doping of 1/4.]

Fig. 4. Charged stripes in the tJ model[37], interpreted as constant hole density domains of variable width. Open circles = average hole density per row; dashed lines = guides to the eye; solid lines = phase separation model.

White and Scalapino[37] have indeed reported evidence for such a phase transition; here we would like to present a reinterpretation of their data, Fig. 4a of Ref. [37]. Since the stripes are sensitive to boundary conditions, we prefer to look at the average hole density along each row (parallel to the stripes) of the simulation, Fig. 4. The data (open circles) fall very close to the form expected for a phase separation model (solid lines), with the same average densities as at 1/8 filling, but now the magnetic stripes retain their minimum width, while the hole-doped stripes get wider. Since 0.18 is close to optimal doping, the optimally doped materials are likely to be character-

ized by a set of widely separated magnetic ladders, with little residual interaction. The physics will be dominated by the physics of the hole-doped stripes at their special doping.

This is bad news for the tJ model. It was specifically designed as a highly simplified model, which retained just enough physics to accurately describe the cuprates near the insulating phase at half filling. It is highly unlikely that the neglect of the oxygens and electron-phonon interactions will continue to be valid in the new hole-doped phase.

We would like to thank A.M. Gabovich for useful discussions about tunneling, and NATO for enabling him to visit us. Publication 743 of the Barnett Institute.

REFERENCES

1. R. S. Markiewicz, *Mod. Phys. Lett. B***1**, 187 (1987).
2. R. S. Markiewicz, *J. Phys. Chem. Sol.*, **58**, 1179 (1997).
3. R. S. Markiewicz, in "High Temperature Superconductors", ed. by M. B. Brodsky, *et. al.*, (Pittsburgh, MRS, 1988), p. 411.
4. E. L. Nagaev, "Physics of Magnetic Semiconductors" (Moscow, Mir, 1983).
5. R. S. Markiewicz, *Physica C***162-164**, 235 (1989); *J. Phys. Cond. Matt.* **2**, 665 (1990).
6. R. S. Markiewicz, *Physica C***153-155**, 1181 (1988).
7. Y. J. Uemura, *et al.*, *Phys. Rev. Lett.* **62**, 2317 (1989).
8. R. S. Markiewicz and B. C. Giessen, *Physica C***160**, 497 (1989).
9. J.D. Jorgensen, *et. al., Phys. Rev. B***38**, 11337 (1988).
10. A. Kampf and J. Schrieffer, *Phys. Rev. B***42**, 7967 (1990).
11. W. Putikka, *et al.*, to be published, *J. Phys. Chem. Sol.* **59** (cond-mat/9803141).
12. R S. Markiewicz, *Physica C***193**, 323 (1992).
13. R S. Markiewicz, *Physica C***200**, 65 (1992), **210**, 235 (1993), and **207**, 281 (1993).
14. J. W. Loram, *et. al., Phys. Rev. Lett.* **71**, 1740 (1993).
15. R. S. Markiewicz, *Phys. Rev. Lett.* **73**, 1310 (1994).
16. D. S. Marshall, *et al.*, *Phys. Rev. Lett.* **76**, 4841 (1996); A. G. Loeser, *et al.*, *Science* **273**, 325 (1996); H. Ding, *et al.*, *Nature* **382**, 51 (1996).
17. J. M. Tranquada, *et al.*, *Nature* **375**, 561 (1995).
18. R. S. Markiewicz, *J. Supercond.* **10**, 333 (1997); *Phys. Rev. B***56**, 9091 (1997).
19. I. Affleck and J. B. Marston, *Phys. Rev. B***37**, 3774 (1988); R. B. Laughlin, *J. Phys. Chem. Sol.* **56**, 1627 (1995); X.-G. Wen and P. A. Lee, *Phys. Rev. Lett.* **76**, 503 (1996).
20. Ch. Renner, *et al., Phys. Rev. Lett.* **80**, 149 (1998).
21. N. Miyakawa, *et al., Phys. Rev. Lett.* **80**, 157 (1998).
22. R. S. Markiewicz, *Physica C***169**, 63 (1990).
23. R. S. Markiewicz and C. Kusko, unpublished (cond-mat/-9802079); R.S. Markiewicz, C. Kusko, and V. Kidambi, unpublished.
24. C. A. Balseiro and L. M. Falicov, *Phys. Rev. B***20**, 4457 (1979).
25. J. Y. T. Wei, *et al., Phys. Rev. B***57**, 3650 (1998).
26. H. Ding, *et. al.,* to be published, *J. Phys. Chem. Sol.* **59** (cond-mat/9712100).
27. A. I. Solomon and J. L. Birman, *J. Math. Phys.* **28**, 1526 (1987).
28. R. S. Markiewicz and M. T. Vaughn, to be published, *J. Phys. Chem. Sol.* **59** (cond-mat/9709137), and *Phys. Rev. B***57**, 14052 (1998).
29. S.-C. Zhang, *Science* **275**, 1089 (1997).
30. C. N. Yang and S.-C. Zhang, *Mod. Phys. Lett. B***4**, 759 (1990).
31. X.-G. Wen and P. A. Lee, *Phys. Rev. Lett.* **80**, 2193 (1998).
32. H.-H. Lin, *et al.*, unpublished (cond-mat/9801285).
33. C. Kusko, R.S. Markiewicz, and M. T. Vaughn, unpublished.
34. H. J. Schulz, *Phys. Rev. B***39**, 2940 (1987).
35. S. R. White and D. J. Scalapino, *Phys. Rev. Lett.* **80**, 1272 (1998).
36. H. Tsunetsugu, *et al. Phys. Rev. B***51**, 16456 (1995).
37. S. R. White and D. J. Scalapino, unpublished (cond-mat/9801274).

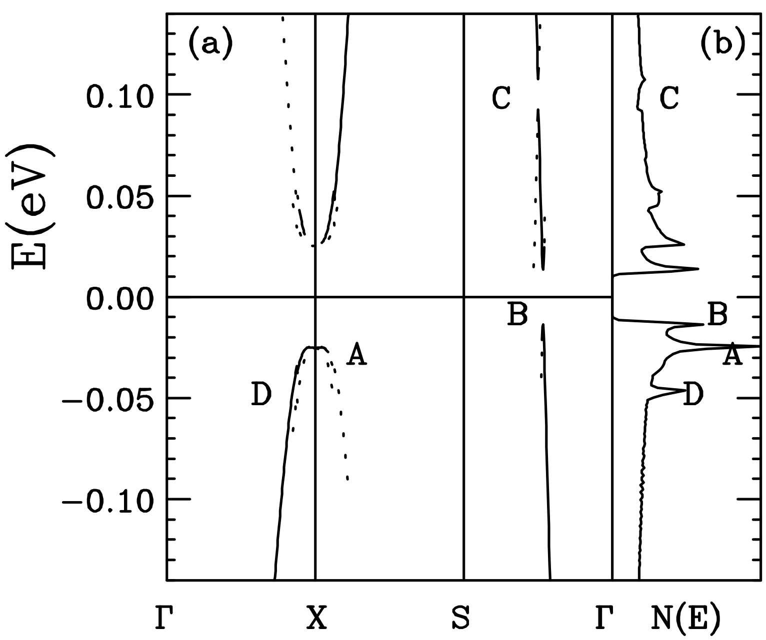

(a)
(b)
E(eV)
0.10
0.05
0.00
−0.05
−0.10
C
B
A
D
C
B
A
D
Γ
X
S
Γ
N(E)

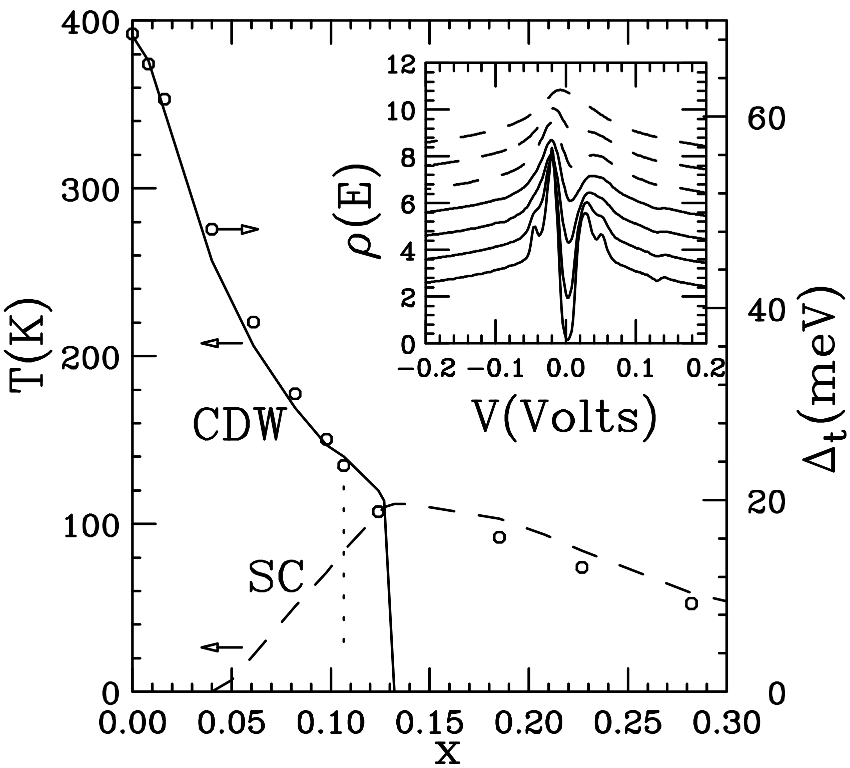

T(K)
x
Δ_t(meV)
CDW
SC
ρ(E)
V(Volts)

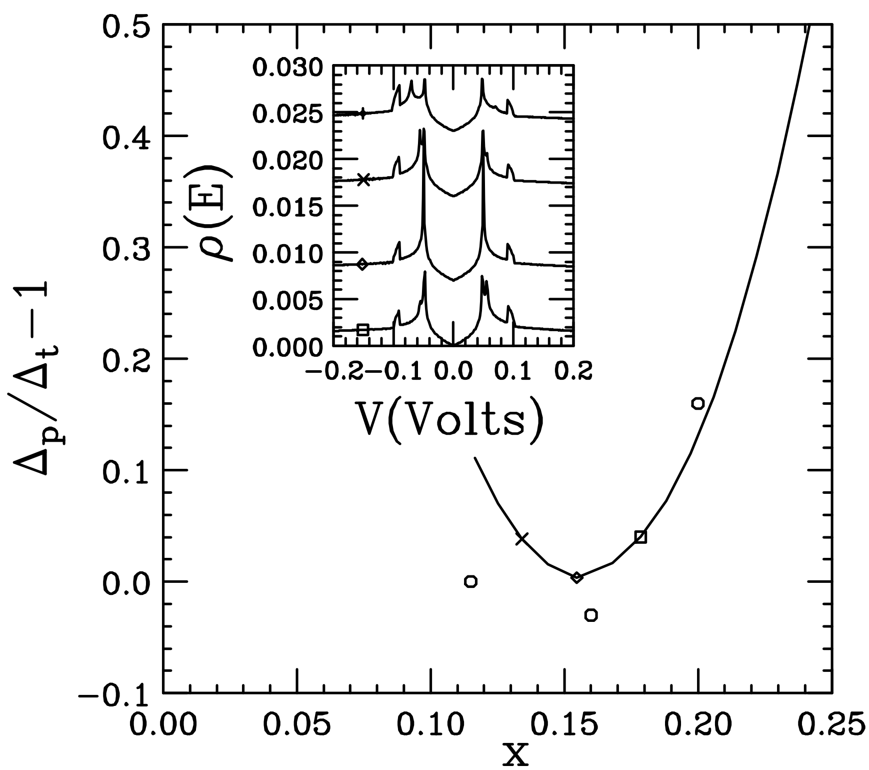

0.5
0.4
0.3
0.2
0.1
0.0
−0.1
Δ_p/Δ_t-1
0.00
0.05
0.10
0.15
0.20
0.25
x
0.030
0.025
0.020
0.015
0.010
0.005
0.000
$\rho(E)$
−0.2
−0.1
0.0
0.1
0.2
V(Volts)

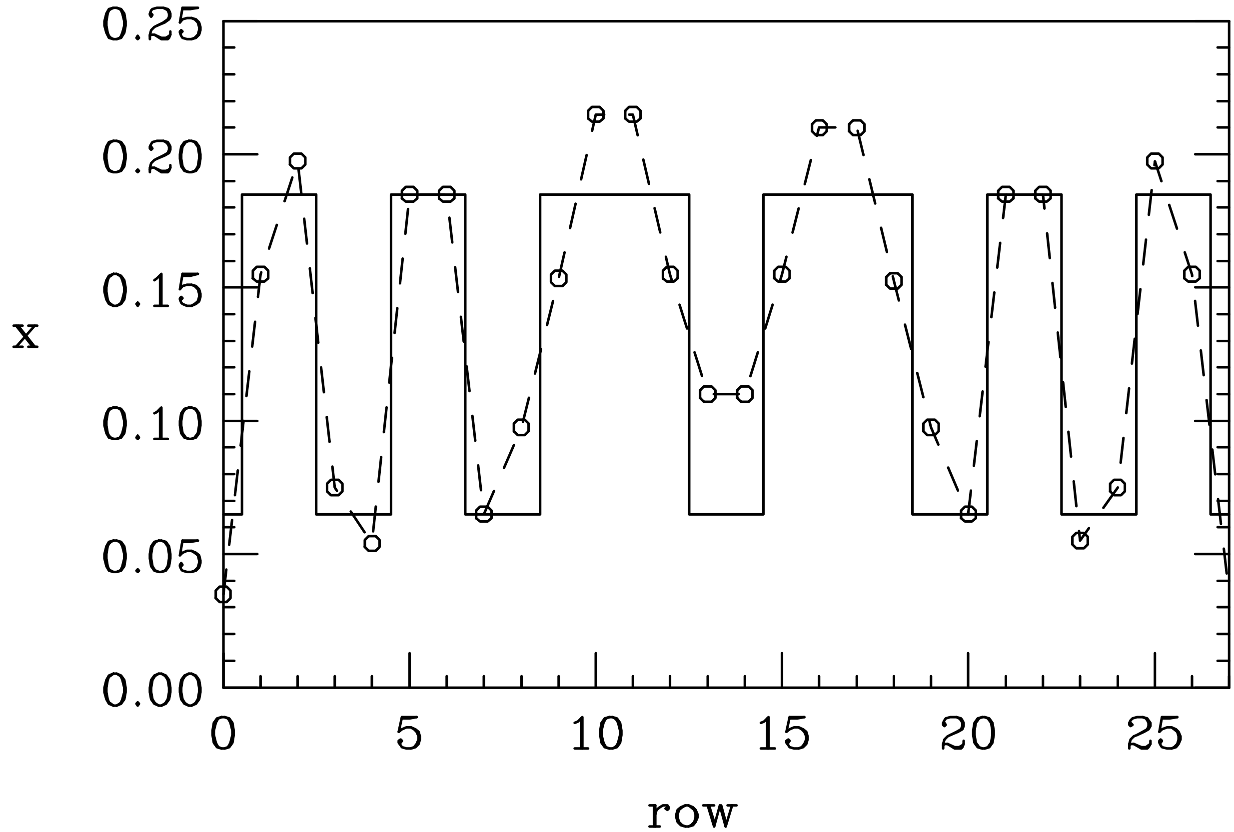

0.25
0.20
0.15
0.10
0.05
0.00
x
0
5
10
15
20
25
row